11th International Conference on Vibration Problems
Z. Dimitrovová *et.al.* (eds.)
Lisbon, Portugal, 9–12 September 2013

EXPERIMENTAL INVESTIGATION OF CENTRIFUGAL PENDULUM VIBRATION ABSORBERS

J. Mayet*[1], D. Rixen[2] and H. Ulbrich[3]

[1,2,3]Institute of Applied Mechanics, Technische Universität München, 85748, Garching, Germany
[1]mayet@amm.mw.tum.de , [2]rixen@tum.de, [3]ulbrich@tum.de

Keywords: CPVA, Vibration Absorbers, Hybrid Control, Experimental Dynamics.

Abstract. *An experimental setup for testing centrifugal pendulum absorbers is described. Centrifugal pendulum vibration absorbers are used for attenuation of torsional vibrations in rotating and reciprocating machines. Typical torque excitations, arising in applications, are generated by using an electric motor with which performance for a broad operating range can be evaluated. A hybrid controller design, which solves the conflict of simultaneous speed maintenance and torque generation, is proposed. Theoretical predictions are confirmed by experimental results of steady-state behavior. Transient responses of a novel absorber are illustrated.*

1 INTRODUCTION

Centrifugal pendulum vibration absorbers (CPVAs), as illustrated in Fig. 2, are used in rotatory machinery for the attenuation of torsional vibrations. In classical applications, including helicopter rotors, radial aircraft engines and combustion engines, the absorbers are designed to have almost order tuned linear dynamical behavior when oscillating about their equilibrium positions. Previous investigations [3] showed that centrifugal absorber devices may experience instabilities resulting in asynchronous responses that are detrimental to the system. In addition, imperfections among the pendula may cause undesirable high amplitude vibrations of single pendula and it is well known that such responses are avoided by slightly detuning the absorbers at the expense of effectiveness [2]. The narrow parameter ranges, where qualitatively different dynamical behavior occurs, do not allow for completely theoretical predictions. As a result, optimal and robust designs have to be thoroughly studied experimentally.

Due to compact designs of the overall system, it is usually not possible to measure the absorber vibration amplitudes and thus to precisely determine the dynamic behavior. Therefore, it is vital to develop a testing apparatus which allows different operating conditions and easy access to measurement points. The benefit of such accessible testing apparatuses is usually counterbalanced by the difficulty of reproducing the time-varying torque necessary to represent excitations encountered in the real application with an electric motor. The applied alternating torque can be written as a limited order Fourier series and by feedback of the electric motor current, the required torque command signal is accurately generated. If, however, it is required to maintain the average speed of the rotor at the same time, the control law has to deal with conflicting goals. Imagine that the absorber is not mounted and only the average speed of a rigid rotating shaft excited by an external disturbing torque has to be maintained. Since an applied torque always causes a change of angular velocity of the shaft, a perfect speed controller would completely counteract the external torque.

Therefore, a specialized speed controller, only maintaining the average speed and simultaneously allowing deviations during a specified time duration, has to be designed. The basic idea of the applied control law, satisfying this requirement, is a decomposition into an angle-discrete, respectively time-discrete and a continuous control signal.

In this paper, an experimental facility for centrifugal absorbers is outlined. Steady-state responses of the absorber are presented and the performance of the controller is investigated. Furthermore, transient responses, where fast changes in the averaged rotation speed under torsional torque excitation occur, are presented.

2 EXPERIMENTAL FACILITY

The experimental setup, schematically shown in Fig. 1, is basically a servomotor driving a rotor on which various test objects can be mounted. The main features are: the response of the test object is contactlessly measured using a rotational Laser Doppler Vibrometer (LDV) and/or a high-speed camera. Polytec's rotational vibrometer RLV-5500 requires no mounted sensors or telemetry and measures absolute angular velocities of rotating structures from 0 to $20000\,[\mathrm{rpm}]$ with $10\,[\mathrm{kHz}]$ bandwidth. Test objects consisting of multiple absorbers are qualitatively studied by using the high-speed camera. Further, a $1024\,[\mathrm{pulse/rev}]$ optical encoder measures the angular velocity of the rotor and the strain gauge sensor measures the torsional torque (see Fig. 1). Taking advantage of the angular velocity and torsional torque measurements of the electric motor as well as mounting a simple flywheel as test object, the parameters of a model describing the experimental setup have been identified and the sensors have been calibrated carefully. For security reasons the operating range is restricted to angular velocities below $1500\,[\mathrm{rpm}]$. In addition to the necessary electric components, Matlab®/Simulink®and dSpace (DS1103 PPC Controller Board, Connector Panel CLP1103 and ControlDesk®) are used on a personal computer.

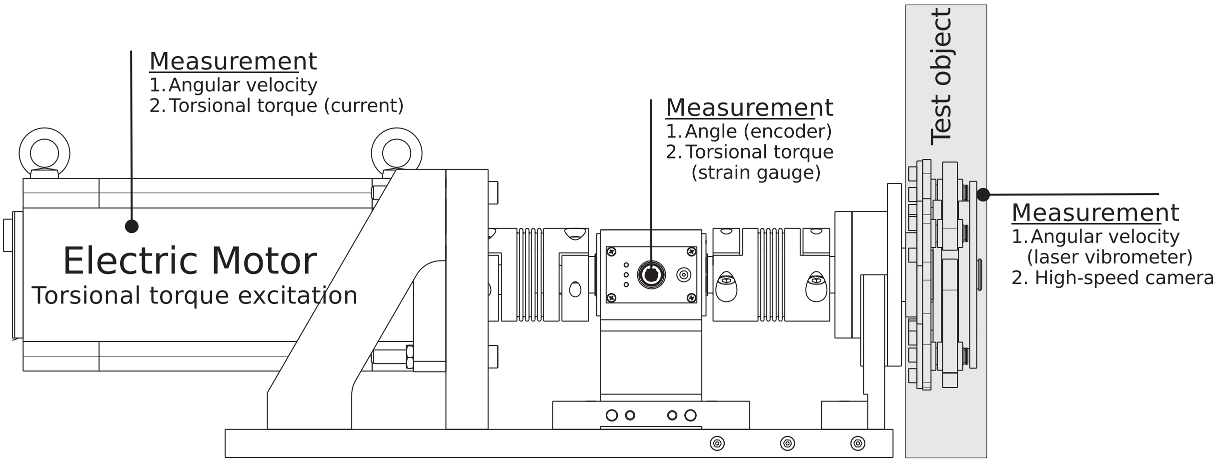

Figure 1: Schematic diagram of the experimental setup.

3 CENTRIFUGAL PENDULUM ABSORBERS

The experimental setup is designed for the identification of centrifugal pendulum vibration absorbers (CPVAs), schematically shown in Fig. 2(a). The absorber is mounted on a rotor (drive shaft) rotating with angular velocity $\dot{\psi} \gg 1\,[\mathrm{rpm}]$ and the absorber is able to perform movements α relative to the rotor. Due to the centrifugal force, the absorber center of mass is relatively accelerated with respect to a rotor-fixed frame of reference with origin on the rotation axis to positions of maximal radial distance, the vertex, respectively equilibrium position. Oscillations of the absorber about its equilibrium position cause a torsional torque acting on the rotor which can counteract external torque excitations. In case of a rotor running at mean angular velocity Ω_0, the oscillation frequency for small absorber responses is approximately proportional to Ω_0 and the proportional constant is obtained from a geometric relationship. For a detailed information on CPVAs the reader is referred to [5, 4, 1, 10].

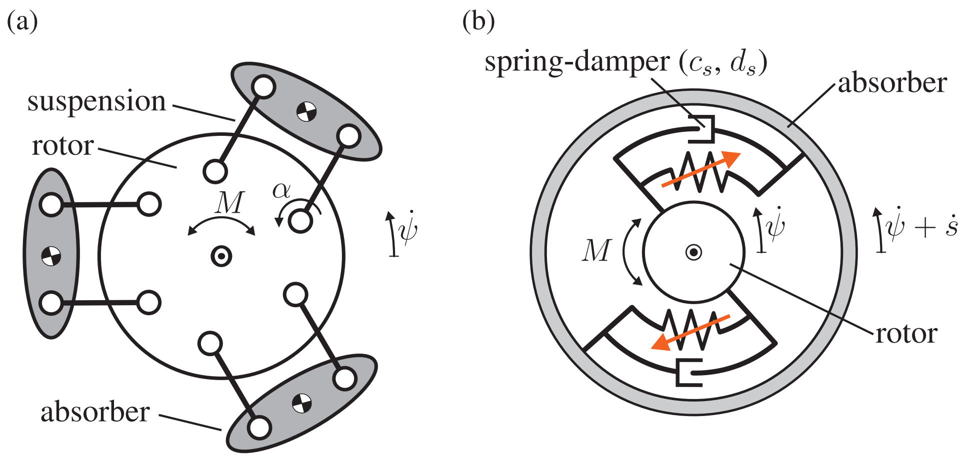

Figure 2: Schematic CPVA: (a) Bifilar pendulum absorber [10]; (b) Linear simplified system.

In this paper, a simplified model for CPVAs, the one degree of freedom linear, parameter-invariant (LPV) system, as illustrated in Fig. 2(b), is addressed for theoretical calculations. The simplified model is basically the well-known linear torsional vibration absorber primarily consisting of an absorber (moment of inertia J_a), the rotor (moment of inertia J_r) and a linear spring-damper element as a connecting component. However, as indicated by arrows in Fig. 2(b), the spring constant c_s is proportional to Ω_0^2. Including linear viscous damping (damping constant d_ψ) of the rotor, applying a speed control torque M_c as well as a periodic excitation torque $M(t)$ acting on the rotor, the simplified system obtained by linearization of a CPVA at $(\psi = 0, \dot{\psi} = \Omega_0, s = 0, \dot{s} = 0)$ is described by

$$\begin{bmatrix} J_\mathrm{r} + J_\mathrm{a} & J_\mathrm{a} \\ J_\mathrm{a} & J_\mathrm{a} \end{bmatrix} \begin{bmatrix} \ddot{\psi} \\ \ddot{s} \end{bmatrix} + \begin{bmatrix} d_\psi & 0 \\ 0 & d_s \end{bmatrix} \begin{bmatrix} \dot{\psi} \\ \dot{s} \end{bmatrix} + \begin{bmatrix} 0 & 0 \\ 0 & J_\mathrm{a}(k\Omega_0)^2 \end{bmatrix} \begin{bmatrix} \psi \\ s \end{bmatrix} = \begin{bmatrix} M(t) + M_c \\ 0 \end{bmatrix}, \quad (1)$$

where the stiffness $c_s = J_\mathrm{a}(k\Omega_0)^2$ with additional constant k, obtained from geometrical relationships is used. Fig. 3 illustrates the frequency response of the LPV system Eq. (1) for numerical values of the parameters given in Tab. 1.

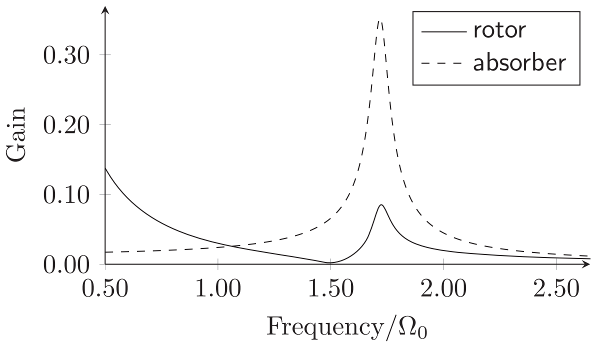

Figure 3: Frequency response.

Parameter	Value	Unit
J_r	$7.711 \cdot 10^{-3}$	$\mathrm{kg\,m^{-2}}$
J_a	$2.430 \cdot 10^{-3}$	$\mathrm{kg\,m^{-2}}$
Ω_0	$\frac{2\pi}{60} \cdot 500$	$\mathrm{rad\,s^{-1}}$
k	1.5	–
d_ψ	$4.4 \cdot 10^{-2}$	Nm s/rad
d_s	$5.0 \cdot 10^{-3}$	Nm s/rad

Table 1: Numerical system values.

As Fig. 3 indicates, a stimulus of the form $M(t) = M_0 \sin(k\Omega_0 t)$ acting on the rotor barely causes rotor oscillations which implies an anti-resonance at a frequency approximately equal to $k\Omega_0$. Therefore, the investigation of CPVAs for torque excitations $M(t) = M_0 \sin(k_\mathrm{E}\Omega_0 t)$ with excitation orders $k_\mathrm{E} \approx k$ are of main interest. In the field of main application, e.g. combustion engines, the torque excitation is synchronous with the rotor angle ψ and contains higher excitation orders. Therefore, the torque excitation can formally be written as

$$M(\psi) = \sum_{i=0}^{N} M_i \sin\left((i+1)k_\mathrm{E}\psi + \varphi_i\right) \qquad N \in \mathbb{N}_0. \quad (2)$$

Due to the different dependencies of the excitations $M(t)$ and $M(\psi)$ with $N = 0$ and $\varphi_0 = 0$, the system responses are in general not comparable but with the assumption $\psi \approx \Omega_0 t$, which implies sufficiently small excitation torque amplitudes, the linear theory can be used for appropriate estimates in many cases.

4 CONTROLLER DESIGN

In this work linear theory will be used for a feedback control design. Experimental results suggest that the controller is applicable to many other test scenarios. We concentrate on oscillations of the absorbers caused by torsional torque excitations acting on the rotor at a specified mean angular velocity of the rotor. Fig. 4 illustrates the feedback control system. It is assumed that the regulated drive as well as the sensor can be treated as gains with a gain factor equal to one and that disturbances are negligible. The required rapid changing command signal $M(t)$ acts on the set value of the current (continuous) controller of the electric motor. Adding a slowly varying command signal M_c, output of the discrete controller, allows to maintain the angular velocity of the rotor without affecting the fast oscillations excited by $M(t)$. Due to the assumptions of an ideal regulated drive, the torsional torque acting on the rotor is equal to the sum of the command signals $M(t)$ and M_c.

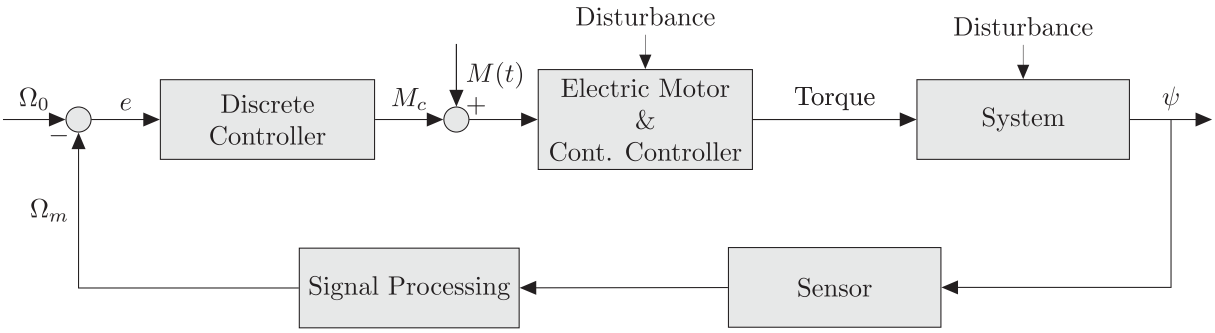

Figure 4: Feedback control system block diagram.

In contrast to continuous control designs for average speed maintenance, where the angular velocity is passed through a low-pass filter [6, 7], a controller design which combines a discrete and continuous approach is presented. Compared with the continuous controller approach an improved command and disturbance behavior is achieved. Since the continuous torque controller can be designed using elementary control theory, only the design of the discrete controller is considered. An introduction and advanced methods related to hybrid systems theory can be found in [8].

4.1 STATE-SPACE MODEL

Rewriting the system given in Eq. (1) as a state-space model gives

$$\frac{\mathrm{d}}{\mathrm{d}t}\begin{bmatrix}\dot{\psi}-\Omega_0\\ s\\ \dot{s}\end{bmatrix} = \underbrace{\begin{bmatrix}a_{11} & a_{12} & a_{13}\\ 0 & 0 & 1\\ a_{31} & a_{32} & a_{33}\end{bmatrix}}_{\mathbf{A}_S}\underbrace{\begin{bmatrix}\dot{\psi}-\Omega_0\\ s\\ \dot{s}\end{bmatrix}}_{\mathbf{x}} + \underbrace{\begin{bmatrix}b_{11}\\ 0\\ b_{31}\end{bmatrix}}_{\mathbf{b}_S}\left(M(t)+M_c-d_\psi\Omega_0\right), \qquad (3)$$

where the constant coefficients are obtained by basic matrix computations. Superimposition of a state space vector $\tilde{\mathbf{x}}$ defined by

$$\tilde{\mathbf{x}} = \tilde{\mathbf{x}}_c\cos(k_E\Omega_0 t) + \tilde{\mathbf{x}}_s\sin(k_E\Omega_0 t) \quad \text{with} \quad \begin{bmatrix}-k_E\Omega_0\mathbf{I} & -\mathbf{A}_S\\ -\mathbf{A}_S & k_E\Omega_0\mathbf{I}\end{bmatrix}\begin{bmatrix}\tilde{\mathbf{x}}_c\\ \tilde{\mathbf{x}}_s\end{bmatrix} = \begin{bmatrix}\mathbf{b}_S M_0\\ \mathbf{0}\end{bmatrix}, \qquad (4)$$

representing oscillations due to the torque excitation $M(t) = M_0\sin(k_E\Omega_0 t)$ and a residual state space vector $\bar{\mathbf{x}}$ satisfying

$$\dot{\bar{\mathbf{x}}} = \mathbf{A}_S\bar{\mathbf{x}} + \mathbf{b}_S\left(M_c - d_\psi\Omega_0\right), \qquad (5)$$

finally gives a solution for Eq. (3) with state space vector $\mathbf{x} = \bar{\mathbf{x}}+\tilde{\mathbf{x}}$ as the sum of the previously defined state space vectors. In order to avoid a feedback of $\tilde{\mathbf{x}}$, an adjusted signal processing of the measured signal ψ is implemented. The signal processing block in Fig. 4 contains a prefilter of the measured signal and a derivative element in order to obtain a good estimate of the angular velocity of the rotor. Assuming that the angular velocity can be measured directly, the system output equation can be written as

$$\dot{\psi} = \begin{bmatrix} 1 & 0 & 0 \end{bmatrix} \mathbf{x} + \Omega_0. \tag{6}$$

As it is not possible to measure $\bar{\mathbf{x}}$ directly, the output Ω_m of the signal processing block is chosen to be the average value of the angular velocity defined by

$$\Omega_m = \frac{1}{T} \int_{t_0}^{t_0+T} \dot{\psi}(\tau) \mathrm{d}\tau. \tag{7}$$

If the averaging period T is an integer multiple n of the oscillation period ($T = \frac{2\pi n}{\Omega_0 k_E}$),

$$\Omega_m = \frac{1}{T} \int_{t_0}^{t_0+T} \dot{\psi} \mathrm{d}\tau = \frac{1}{T} \begin{bmatrix} 1 & 0 & 0 \end{bmatrix} \int_{t_0}^{t_0+T} \mathbf{x} \mathrm{d}\tau + \Omega_0 = \frac{1}{T} \begin{bmatrix} 1 & 0 & 0 \end{bmatrix} \int_{t_0}^{t_0+T} \bar{\mathbf{x}} \mathrm{d}\tau + \Omega_0, \tag{8}$$

is obtained. Due to the particular choice of Ω_m in Eq. (8), the resulting feedback only contains the state space vector $\bar{\mathbf{x}}$ which allows to consider the system defined by Eq. (5) for the discrete controller design and the analysis of the resulting closed loop system. In order to approximately satisfy the assumption of an ideal regulated drive, artificial dynamic behavior of the discrete controller is defined by

$$x_c = M_c - d_\psi \Omega_0 \qquad \begin{bmatrix} \dot{x}_c \\ \ddot{x}_c \end{bmatrix} = \underbrace{\begin{bmatrix} 0 & 1 \\ -k_c & -d_c \end{bmatrix}}_{\mathbf{A}_C} \begin{bmatrix} x_c \\ \dot{x}_c \end{bmatrix} + \underbrace{\begin{bmatrix} 0 \\ k_c \end{bmatrix}}_{\mathbf{b}_C} u\,, \tag{9}$$

where u is the input and k_c, respectively d_c are design parameters. In the following section 4.2, the (discrete) input u is defined by the input $e = \Omega_0 - \Omega_m$ of the discrete controller. The overall state space model is then given by

$$\frac{\mathrm{d}}{\mathrm{d}t} \begin{bmatrix} \bar{\mathbf{x}} \\ x_c \\ \dot{x}_c \end{bmatrix} = \underbrace{\begin{bmatrix} \mathbf{A}_S & \mathbf{b}_S \begin{bmatrix} 1 & 0 \end{bmatrix} \\ \mathbf{0} & \mathbf{A}_C \end{bmatrix}}_{\mathbf{A}} \underbrace{\begin{bmatrix} \bar{\mathbf{x}} \\ x_c \\ \dot{x}_c \end{bmatrix}}_{\mathbf{z}} + \underbrace{\begin{bmatrix} \mathbf{0} \\ \mathbf{b}_C \end{bmatrix}}_{\mathbf{b}} u \tag{10}$$

and the error e can be written as

$$e = \Omega_0 - \Omega_m = -\frac{1}{T} \underbrace{\begin{bmatrix} 1 & 0 & 0 & 0 & 0 \end{bmatrix}}_{\mathbf{c}^T} \int_{t_0}^{t_0+T} \mathbf{z} \mathrm{d}\tau. \tag{11}$$

4.2 PI-CONTROLLER

After the implementation of various continuous controllers and evaluation of the command and disturbance behavior, we found that a discrete control design achieves the requirements best. During the sampling period $T = \frac{2\pi n}{\Omega_0 k_\mathrm{E}}$, the input u is kept constant and the discretization of system Eq. (10) leads to

$$\mathbf{z}_{k+1} = e^{\mathbf{A}T} \mathbf{z}_k + \mathbf{A}^{-1} \left(e^{\mathbf{A}T} - \mathbf{I} \right) \mathbf{b} u_k, \tag{12}$$

where the index k indicates an instant of time $t = t_k = kT$. The discrete PI-controller with integral gain k_i and proportional gain k_p is defined as:

$$u_k = u_{k-1} + (\alpha T k_i + k_p)\, e_k + ((1-\alpha)\, k_i T - k_p)\, e_{k-1} \tag{13}$$

where

$$e_k = -\frac{1}{T}\mathbf{c}^T \int_{t_k}^{t_k+T} \mathbf{z}\mathrm{d}\tau = -\frac{1}{T}\mathbf{c}^T \int_{t_k}^{t_k+T} e^{\mathbf{A}(t-t_k)}\mathbf{z}_{k-1} + \mathbf{A}^{-1}\left(e^{\mathbf{A}(t-t_k)} - \mathbf{I}\right)\mathbf{b}u_{k-1}\mathrm{d}\tau \tag{14}$$

$$= \frac{1}{T}\mathbf{c}^T\mathbf{A}^{-1}\left[\left(\mathbf{I} - e^{\mathbf{A}T}\right)\mathbf{z}_{k-1} + \left(\mathbf{A}^{-1}\left(\mathbf{I} - e^{\mathbf{A}T}\right) + T\mathbf{I}\right)\mathbf{b}u_{k-1}\right] \tag{15}$$

$$e_{k-1} = \frac{1}{T}\mathbf{c}^T\mathbf{A}^{-1}\left[\left(\mathbf{I} - e^{\mathbf{A}T}\right)\mathbf{z}_{k-2} + \left(\mathbf{A}^{-1}\left(\mathbf{I} - e^{\mathbf{A}T}\right) + T\mathbf{I}\right)\mathbf{b}u_{k-2}\right], \tag{16}$$

and $\alpha \in \{1, 1/2\}$ allowing to use either a trapezoidal integration rule ($\alpha = 1/2$) or Euler's integration method ($\alpha = 1$). Using Eqs. (12), (13), (15) and (16) as well as rearranging terms, the closed loop system can be formally written as

$$\begin{bmatrix}\mathbf{z}_{k-1} & \mathbf{z}_k & \mathbf{z}_{k+1} & u_{k-1} & u_k\end{bmatrix}^T = \mathbf{\Phi}\begin{bmatrix}\mathbf{z}_{k-2} & \mathbf{z}_{k-1} & \mathbf{z}_k & u_{k-2} & u_{k-1}\end{bmatrix}^T \tag{17}$$

where $\mathbf{\Phi}$ is the monodromy matrix of the discrete system. Fig. 5 illustrates the eigenvalues of the monodromy matrix $\mathbf{\Phi}$ for the specified numerical values of the design parameters. The closed loop system is asymptotically stable since all eigenvalues are inside the unit circle. Further, a comparison of the different integration rules by choosing α is used to decide whether the integration time T and the associated errors are sufficiently small.

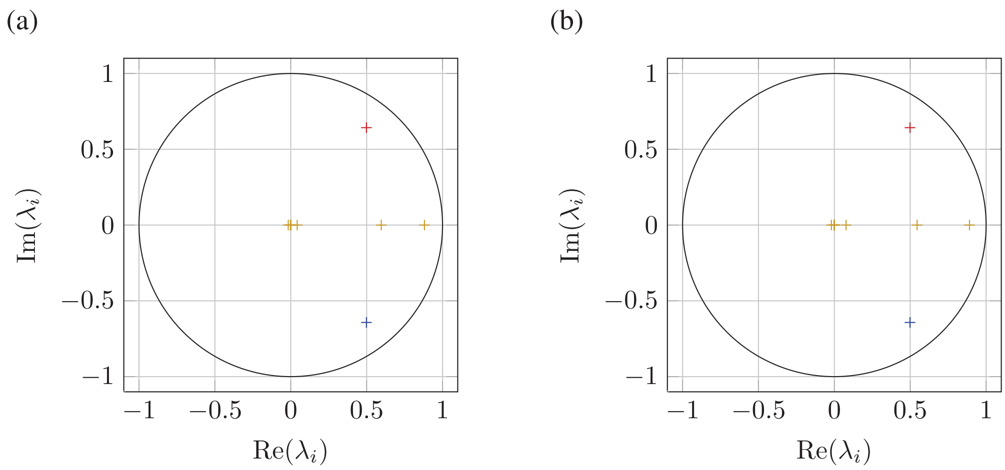

Figure 5: Eigenvalues of matrix $\mathbf{\Phi}$: (a) Trapezoidal rule $\alpha = 1/2$; (b) Euler's method $\alpha = 1$; Parameters: $n = 1$, $k_i = 0.1$, $k_p = 0.008$, $k_c = 2 \cdot 10^4$, $d_c = 250$ and the numerical system values given in Tab. 1.

4.2.1 ANGLE-DISCRETE PI-CONTROLLER

As the excitation torque in the field of main application is synchronous with the rotor angle ψ, the system defined in Eq. (1) is nonlinear if $M(t)$ is replaced by $M(\psi)$. However, the assumption of sufficiently small fluctuations of the angular velocity of the rotor, implying small torque excitation amplitudes, allows to compare the nonlinear system behavior with the linear system behavior. Therefore, the only difference to the previous approach is an angle-based discretization: the value u of the control signal is updated every $\Delta\psi = 2\pi n/k_{\mathrm{E}}$ radians and the averaged value of the rotor angular velocity, which is necessary to calculate u_{k+1}, is obtained by integration over the time interval $[t(\psi_k), t(\psi_k + 2\pi n/k_{\mathrm{E}})]$. Experimental results confirmed that the resulting controller is stable and more importantly that the control torque M_c is nearly constant for steady-state.

5 EXPERIMENTAL RESULTS

In this section, experimental results of steady-state as well as transient responses are presented. In general, steady-state investigations are mainly done to estimate the performance of the absorber and to locate phenomena where qualitatively different system behavior occurs. Transient responses are directly related to the field of application. As an example, automotive applications require robustness of the absorbers against engine accelerations.

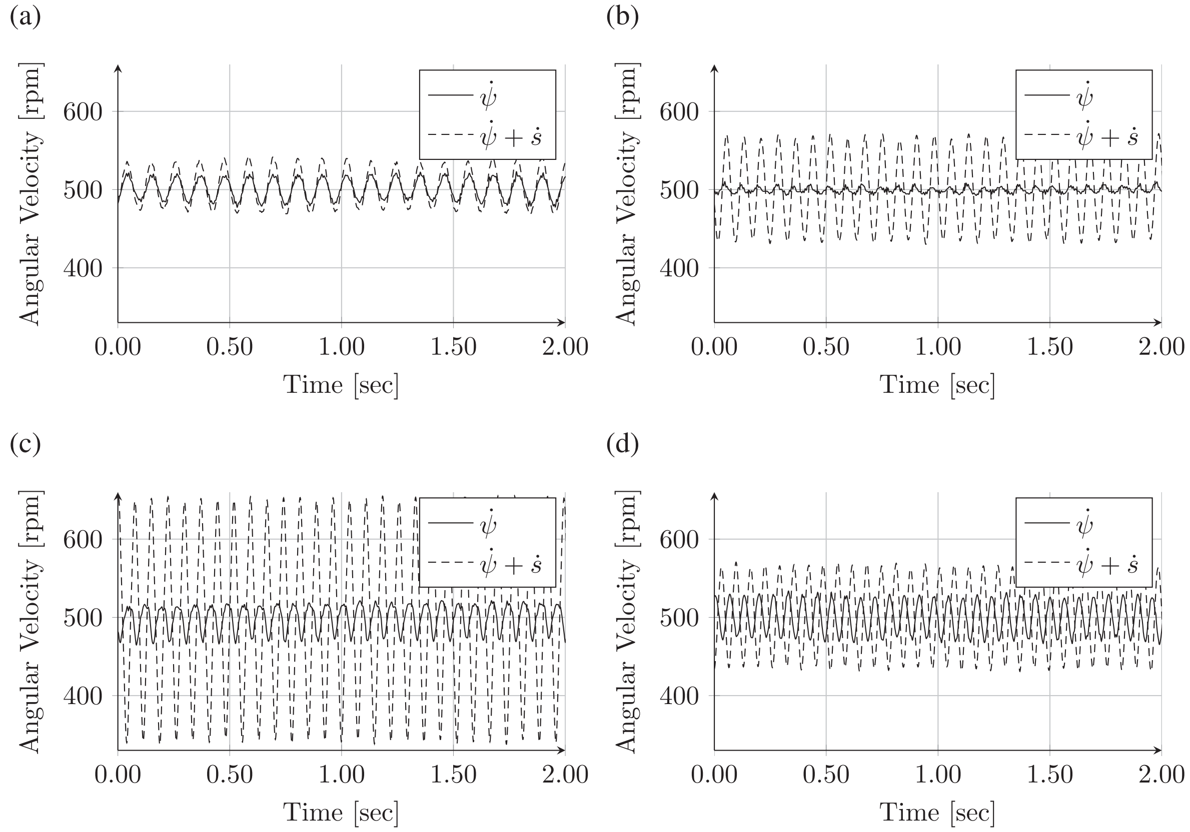

Figure 6: Steady-state responses for different excitation orders k_{E} with torque amplitude $M_0 = 7.0\,[\mathrm{Nm}]$: (a) $k_{\mathrm{E}} = 1.11$; (b) $k_{\mathrm{E}} = 1.55$; (c) $k_{\mathrm{E}} = 1.625$; (d) $k_{\mathrm{E}} = 1.850$.

The test object, called synchronous centrifugal pendulum absorber (SCPA), mounted during test executions is a single degree of freedom absorber. Despite a mechanism generating the stiffness c_s, the system can be thought to look like the equivalent system shown in Fig. 2(b). For details on the test object SCPA, the reader is referred to [9, 10].

First, steady-state responses are addressed: the fluctuation torque is a single harmonic $M(\psi) = M_0 \sin(k_{\mathrm{E}}\psi)$ and the rotor is running at a mean angular velocity $\Omega_0 = 500\,[\mathrm{rpm}]$. The absolute velocity $\dot{s} + \dot{\psi}$ of the absorber is measured with the LDV and the rotor angle signal is generated by the encoder. All signals are then passed through a low-pass filter with cutoff frequency at $40\,[\mathrm{Hz}]$. Comparison of Fig. 6 with the frequency response in Fig. 3 indicates qualitatively the same dynamical behavior for this test scenario. The absorber response is in-phase/out-of-phase for k_E below/above values of k and the absorber attenuates torsional vibrations near anti-resonance. Large absorber responses are obtained at higher excitation orders (see Fig. 6(c)) where nonlinear effects become visible. During these experimental investigations, the control torque signal was found to vary approximately $0.05\,[\mathrm{Nm}]$ which is small in contrast to the obtained mean value of $3.6\,[\mathrm{Nm}]$.

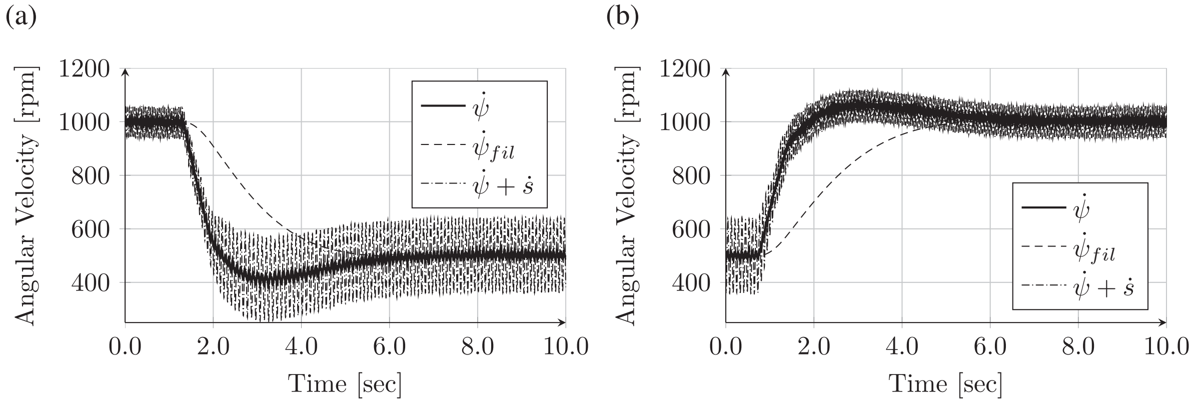

Figure 7: Transient responses for excitation order $k_\mathrm{E} = 1.55$ with torque amplitude $M_0 = 15.0\,[\mathrm{Nm}]$: (a) $1000\,[\mathrm{rpm}] \rightarrow 500\,[\mathrm{rpm}]$; (b) $500\,[\mathrm{rpm}] \rightarrow 1000\,[\mathrm{rpm}]$.

The second scenario are step responses where the set value Ω_0 is $500\,[\mathrm{rpm}]$ before and $1000\,[\mathrm{rpm}]$ after command execution and vice versa. Again, a single harmonic torque $M(\psi) = M_0 \sin(k_\mathrm{E}\psi)$ acts on the rotor and after command execution steady-state is reached within $\Delta t \approx 6\,[\mathrm{sec}]$ for the chosen values of the controller design parameters (see Fig. 7). Note that smaller settling times can be achieved by tuning the controller parameters accordingly. For simplicity, the numerical values, which have been used for steady-state investigations, were retained unchanged. Additionally, the signal $\dot{\psi}_{fil}$, generated by passing $\dot{\psi}$ through a low pass-filter with cutoff frequency at $1\,[\mathrm{Hz}]$, is shown in Fig. 7 in order to illustrate that such transient responses can not be obtained by a control feedback of $\dot{\psi}_{fil}$.

6 CONCLUSIONS

Centrifugal pendulum vibration absorbers were briefly introduced and an experimental setup allowing for systematic investigations on the dynamical behavior of these absorbers was presented in detail. A hybrid time-discrete PI-controller design, which is extended to an efficient angle-discrete controller was implemented. The paper closes with experimental results of a novel centrifugal absorber. It is shown that steady-state responses of the absorber confirm theoretical predictions and the angular velocity of the rotor is accurately maintained. Even transient responses can be studied by the use of the proposed controller. To the best of our knowledge, theoretical investigations of transient step responses have not been considered in the literature so far but first steps in this direction have been made by experimental studies from which important practical performance specifications can be determined. Investigating transient responses of the system in more detail is subject of our future work.

REFERENCES

[1] A S Alsuwaiyan and S W Shaw. Performance and dynamic stability of general-path centrifugal pendulum vibration absorbers. *Journal of Sound and Vibration*, 252(5):791–815, 2002.

[2] A S Alsuwaiyan and S W Shaw. Steady-state responses in systems of nearly-identical torsional vibration absorbers. *Transactions-American Society of Mechanical Engineers Journal of Vibration and Acoustics*, 125(1):80–87, 2003.

[3] C P Chao, C T Lee, and S W Shaw. Non-unison dynamics of multiple centrifugal pendulum vibration absorbers. *Journal of Sound and Vibration*, 204(5):769–794, 1997.

[4] J P Den Hartog. Tuned pendulums as torsional vibration eliminators. *Stephen Timoshenko 60th Anniversary Volume*, pages 17–26, 1938.

[5] H H Denman. Tautochronic bifilar pendulum torsion absorbers for reciprocating engines. *Journal of Sound and Vibration*, 159(2):251–277, 1992.

[6] A G Haddow and S W Shaw. Torsional vibration absorbers: A testing and evaluation apparatus. 2001.

[7] Alan G Haddow and Steven W Shaw. Centrifugal Pendulum Vibration Absorbers: An Experimental and Theoretical Investigation. *Nonlinear Dynamics*, 34(3):293–307, 2003.

[8] Jan Lunze, Françoise Lamnabhi-Lagarrigue, and Others. *Handbook of hybrid systems control: theory, tools, applications*. Cambridge University Press, 2009.

[9] J Mayet and H Ulbrich. Synchronous Centrifugal Pendulum Absorber. *European Mechanics Society 532 Colloquium on time-periodic systems*, 2012.

[10] J. Mayet and H. Ulbrich. Tautochronic Centrifugal Pendulum Vibration Absorbers - General Design and Analysis. *Journal of Sound and Vibration*, submitted, 2013.